

# Energy criterion for modelling damage evolution in cross-ply composite laminates

D.T.G. Katerelos<sup>a,b,\*</sup>, J. Varna<sup>a</sup>, C. Galiotis<sup>b</sup>

<sup>a</sup> Division of Polymer Engineering, Department of Applied Physics and Mechanical Engineering, Luleå University of Technology, SE 971 87 Luleå, Sweden

<sup>b</sup> FORTH/ICE-HT, Stadiou Street, Platani, Patras, P.O. Box 1414, GR-265 04, Greece

Received 23 April 2007; received in revised form 16 September 2007; accepted 24 September 2007

Available online 29 September 2007

## Abstract

The energy dissipated in cross-ply laminates during loading–unloading loops is obtained from stress–strain curves for cross-ply laminates and used in an energy based approach to predict the development of matrix cracking. The dissipated energy is correlated to the crack density growth data recorded for a reference laminate. The critical strain energy release rate,  $G_c$  obtained in this way is increasing with the applied strain. This phenomenon reflects the statistical nature of  $G_c$  distribution in the 90-layer: the first cracks (lower strain) develop in positions with lower fracture toughness. The obtained  $G_c$  data are in a good agreement with fracture toughness data obtained using LEFM based “compliance calibration” model in which the stiffness change with increasing strain is used. Finally, the matrix cracking development is successfully simulated using in the LEFM model, the data for critical strain energy release rate and an earlier derived stiffness–crack density relationship. It has been demonstrated that knowing the laminates geometry and measuring the laminate stiffness reduction with strain or (alternatively measuring the dissipated energy) the damage evolution may be simulated, thus reducing the necessity for optical observations to validation only.

© 2007 Elsevier Ltd. All rights reserved.

**Keywords:** A. Polymer–matrix composites (PMCs); B. Matrix cracking; C. Damage mechanics; C. Fracture mechanics; D. Raman spectroscopy

## 1. Introduction

Damage mechanics is the field intensively developing during the last decades and providing tools for studies of composite materials behaviour after damage initiation. For the damage initiation prediction appropriate strength based criteria could be used. Designing structural elements for functionality in the presence of damage, the above sequence has to be accounted for when structure’s durability is assessed. Damage in laminated composite materials develops in three subsequent and mostly interlaced forms: matrix cracking (intralaminar damage), delaminations

(interlaminar damage) and fibres failure (laminates collapse). The interfaces between the aforementioned damage modes are not well defined, that is matrix cracking may be accompanied with local delaminations and/or fibres breakage. However, intralaminar, or as it is often called, transverse matrix cracking in plies oriented at angles different than the loading axes is considered to appear first. Therefore, during the last 30 years it has been the main subject of studies for many researchers [1–5]. The crack density and damage entity characteristics in terms of damage vectors and tensors, crack opening displacements, etc. were used to quantify the effect of damage on the overall behaviour of laminates [1–7].

Modelling the initiation and development of matrix cracking in a composite system starts with the evaluation of the stresses distributions within the laminate. In the reviews [1–5], all the main different approaches for the stress distribution determination could be found. Since

\* Corresponding author. Address: Division of Polymer Engineering, Department of Applied Physics and Mechanical Engineering, Luleå University of Technology, SE 971 87 Luleå, Sweden. Tel.: +46 (0) 920 491656; fax: +46 (0) 920 491084.

E-mail address: [katerel@pathfinder.gr](mailto:katerel@pathfinder.gr) (D.T.G. Katerelos).

the internal stress state is quantified the intralaminar crack-ing evolution could be modelled. The models proposed may be categorized, according to their basic approaches, into two main groups: strength based models and fracture mechanics based models; see review [4]. Most of the stress based models account for the strength distribution within the laminate and the probability of local failure.

Among physical quantities, used to characterize micro-damage development in laminates due to thermo-mechanical loading, the most often used is the critical strain energy release rate (often erroneously called fracture toughness). It is commonly considered as a material constant; however, an appropriate test for its determination is still an open question. In static crack growth problems, the critical strain energy release rate for the crack growth is either appropriately chosen in order to satisfy experimental damage evolution data [3,14], or derived from cracking data and  $G$  using the stress state provided analytically [15–20] or numerically (finite elements) [21]. The attempts to use measured laminate Young's modulus changes or the measured dissipated energy are more rarely described in the literature.

The strain energy release rate,  $G$ , is usually calculated analyzing the stress state change with increasing crack density or using the change in the calculated elastic modulus of the laminate. Together with independently obtained  $G_c$  it is used to model damage evolution in composite laminates under both static and fatigue loading. Monitoring crack growth under fatigue has been presented by several researchers [9–13], while detailed review can be found in [4]. The  $G_c$  is used in the Paris power law criterion for individual crack growth during cyclic loading [27]. As a crack initiation criterion for composite laminates under static flexure loading,  $G_c$  has been used by Smith and Ogin [22,23]. One example of an approach which incorporates probabilities in the fracture mechanics analysis is the early analytical model proposed by Laws and Dvorak [8]. Statistical  $G_c$  distribution was extensively used by Wang and Chou see for example [27].

In the present paper, the critical strain energy release rate for two glass fibre reinforced epoxy composite systems is derived using the dissipated energy obtained from stress–strain curves recorded during an ordinary loading–unloading tensile test with increasing maximum and using the observed crack density relationship with the applied strain for a reference laminate. As an alternative method for  $G_c$  determination the stiffness reduction with strain is used. The obtained  $G_c$  values strongly depend on the maximum strain level in the loading loop which reflects the statistical nature of the fracture toughness distribution along the 90-ply: the  $G_c$  values for lower strains correspond to cracks in the weakest locations whereas the new cracks appearing at higher strains require more energy. Finally, theoretical predictions of the crack density as a function of applied strain are performed using the obtained  $G_c$  and an analytical model describing the longitudinal modulus degradation as a function of crack density [26].

## 2. Experimental

Two cross-ply glass fibres reinforced composite systems (GFRP) were used for the dissipated energy calculations. The first (GF1) was manufactured using a modified frame-winding technique. Detailed description of the procedure can be found in the literature [6,7]. A steel frame welded at 90° was used for the glass fibres winding with the inner layer wound firstly. Then, the 0° layer was wound. Tensile coupons were cut from the laminates according to ASTM D3039 standard. A Shell “Epicote” 828 resin was used and cured with nadic methyl-anhydride and accelerator K61B in the ratio 100:60:4. The laminate was cured between thick glass plates under 8–10 bar pressure for 3 h at 100 °C, followed by a post-cure at 150 °C for 3 h. The fibre volume fraction of the thus produced plates was 63%, the laminate ply thickness was 0.64-mm for the 0° plies and 0.62-mm for the 90° plies.

In the case of the second composite system (GF2) three different laminates with different ply thicknesses were considered. They were manufactured using a vacuum bag technique from unidirectional prepreps with the commercial code VICOTEX NVE 913/28%/192/EC9756. The laminates were cured at 90 °C for 30 min followed by post-curing at 120 °C for 60 min under 3–7 bar pressure. Three laminates stacking sequences were manufactured, [0/90<sub>4</sub>]<sub>s</sub> (GF2\_1-4), [0/90<sub>2</sub>]<sub>s</sub> (GF2\_1-2) and [0<sub>2</sub>/90<sub>2</sub>]<sub>s</sub> (GF2\_2-2) with an average thickness of 1.35, 0.80 and 1.04 mm, respectively. Specimens were cut according to the ASTM D3039 standard in the reinforcement direction of the outer layers. Specimen edges were polished in order to eliminate any defects that may appear during sawing. It has been proved [24] that edge polishing is the cause for rapid crack propagation, thus the development of cracks covering the full specimen width is expected. Details on the GF2 material manufacturing can be found in [25].

GF1 laminates were subjected to a repeated mechanical tensile testing for the crack pattern development. The mechanical tensile loading was applied through an MTS 858 Mini Bionix tester [6]. The loading rate was 0.1 mm/min to achieve controlled and stable crack growth. An electrical strain gauge has been attached on the specimen in order to control the resulting strain. The specimen was loaded up to a certain strain level and unloaded to zero stress level. Then the procedure was repeated for higher strain levels until reaching the so called crack saturation point. The stress–strain curves thus produced are presented in Fig. 2a. Crack density at each strain level, see the transverse crack appearance in Fig. 1, was monitored using the

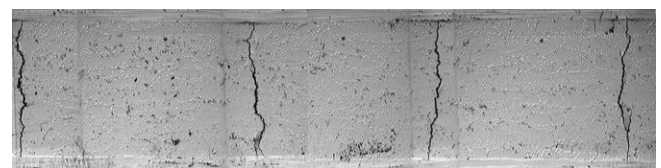


Fig. 1. A typical crack pattern in cross-ply laminates.

technique of laser Raman spectroscopy [6,7]. The initial Young's modulus of the laminate was calculated from the first stress–strain curve provided by the attached strain gauge and the MTS load cell.

GF2 material laminates were tested under quasi-static stepwise tensile loading with an applied displacement rate of 2 mm/min [25]. Loading was periodically interrupted and the specimens were unloaded for measuring the crack density. Crack density was monitored by optical means in transmitted light, which was possible due to the partial transparency of the materials [25]. The applied strain in the loading direction was measured by an extensometer. The Young's modulus at each loading step was derived from the corresponding unloading stress–strain curve within the 0.1–0.3% axial strain range [25].

The two different composite systems subjected to rather different strain rates were used to demonstrate that the suggested methodology is applicable in wide range of materials behaviour. The strain rate for all laminates belonging to same material system was kept constant. Thus the possible effects of more brittle material behaviour at high strain rates and the creep rupture type of effects at low strain rate are included in corresponding values of  $G_c$ . Due to these possible additional effects no comparison of both materials is made.

### 3. Modelling

In a displacement controlled test the critical strain energy release rate,  $G_c$ , is defined by the well-known equation

$$-\frac{\partial U}{\partial A} \Big|_{\varepsilon=\text{constant}} = G_c(\varepsilon) \quad (1)$$

where  $U$  is the strain energy of the specimen, while  $A$  is the total crack surface area formed by all cracks, that is

$$A = Nwh_{90} \quad (2)$$

where  $N$  is the number of cracks formed,  $w$  is the specimen width and  $h_{90}$  is the 90°-layer thickness. The strain energy of the specimen (ignoring thermal stresses which are not large in a glass fibre composite laminates) can be written as

$$U = \frac{E_x}{2} \varepsilon^2 V \quad (3)$$

$E_x$  is the damaged laminate longitudinal Young's modulus,  $\varepsilon$  is the applied strain and  $V$  is the specimen volume

$$V = Lwh \quad (4)$$

$L$  is the specimen length and  $h$  its thickness.

Substituting Eqs. (2)–(4) into Eq. (1) the following expression for  $G_c$  can be extracted

$$-\frac{1}{2} \varepsilon^2 L \frac{h}{h_{90}} \frac{\partial E_x}{\partial N} = G_c(\varepsilon) \quad (5)$$

Crack density,  $\rho$ , is defined as the ratio of the total number of cracks within a length over the length. Thus for the specimen with length,  $L$ , it is

$$\rho = \frac{N}{L} \quad (6)$$

Combining Eqs. (5) and (6)  $G_c$  is expressed as a function of crack density

$$-\frac{1}{2} \varepsilon^2 \frac{h}{h_{90}} \frac{\partial E_x}{\partial \rho} = G_c(\varepsilon) \quad (7)$$

It has been shown from [26] that the dependence of laminate longitudinal Young's modulus,  $E_x$ , on crack density in the damaged cross-ply laminate is of the form

$$E_x = \frac{E_0}{1 + A_0 \rho u(\rho)} \quad (8)$$

where  $E_0$  is undamaged laminate longitudinal Young's modulus,  $A_0$  is a constant which value depends on the model used (ex. shear lag) and  $u(\rho)$  is average crack opening displacement normalized with respect to the far-field stress in the 90-layer. We assume, for the sake of simplicity, that the normalized crack opening does not depend on the distance between cracks

$$u(\rho) = u_0 \quad (9)$$

where the value of  $u_0$  can be calculated by any existing stress model. Actually  $u$  is not a constant and it decreases at high crack density when the interaction between cracks is noticeable. In this paper, the model proposed by Lundmark and Varna [26] is used. Differentiating Eq. (8) and taking into account Eq. (9) the partial derivative of the  $E_x$  with respect to  $\rho$  is calculated. Then Eq. (7) becomes

$$\frac{1}{2} \varepsilon^2 \frac{h}{h_{90}} \frac{E_0}{(1 + A_0 \rho u_0)^2} A_0 u_0 = G_c(\varepsilon) \quad (10)$$

which can be rewritten using Eq. (8) as

$$\frac{1}{2} \varepsilon^2 \frac{h}{h_{90}} E_x^2 \frac{A_0 u_0}{E_0} = G_c(\varepsilon) \quad (11)$$

The constant  $A_0$  as calculated from [26] is given by

$$A_0 = \frac{E_T}{E_0} \frac{2h_{90}}{h_{90} + 2h_0} h_{90} \quad (12)$$

According to the studies performed by Lundmark and Varna [26] the crack opening displacement in an internal layer can be represented by the following power law:

$$u_0 = A_m + B_m \left( \frac{E_T}{E_L} \right)^{n_m} \quad (13)$$

where the constants  $A_m$ ,  $B_m$  and  $n_m$  are given by following empirical forms:

$$\begin{aligned} A_m &= 0.52 \\ B_m &= 0.3075 + 0.1652 \left( \frac{h_{90} - 2h_0}{2h_0} \right) \\ n_m &= 0.030667 \left( \frac{h_{90}}{2h_0} \right)^2 - 0.0626 \left( \frac{h_{90}}{2h_0} \right) + 0.7037 \end{aligned} \quad (14)$$

#### 4. Results – discussion

A “stop-and-go” procedure was employed in the crack forming experimental investigation on both composite systems. The specimen was loaded up to a certain strain level where new cracks formed, while the applied strain was controlled by the strain gauge attached on one side of the specimen (GF1) or the extensometer along the loading direction (GF2). Following, they were unloaded to zero stress, while the residual strain was recorded and the crack pattern was monitored. In the case of GF1 laminate the crack pattern was mapped indirectly through the use of laser Raman spectroscopy for measuring the strain arising within the  $0^\circ$  lamina due to cracking. Details on this method have been referred in previously published works [6,7]. The crack pattern arising in the GF2 laminates at all strain levels and for all types of specimens used was monitored using an optical microscope. This procedure was repeated until the crack forming mode of damage was completed by reaching the so called saturation point. The stress–strain curves are presented in Fig. 2a–d.

The first step in the experimental critical strain energy release rate determination is the calculation of the dissipated energy,  $U_d$ , at each loading–unloading cycle. By integrating the loading stress–strain curve the energy,  $U_l$ , given to the material is calculated, which includes both the strain energy and the additional work performed on additional

displacements due to increase of the total crack area. The integration of the unloading curve corresponds to the energy returned,  $U_u$ . The difference between these two values represents the total dissipated energy,  $U_d$ , in each loading cycle

$$U_d = U_l - U_u \quad (15)$$

The dissipated energy differs from the mechanical strain energy  $U$  introduced in the previous section. It includes also viscoelastic effects as well as reduction of strain energy related to thermal stresses as a consequence of thermal stress relaxation due to cracking. The latter phenomenon results in small permanent tensile strains after each loading–unloading cycle. The additional work performed by the external load related to additional macro-scale displacements due to the cracks growth is also included.

The dissipated energy for both materials systems as a function of the maximum applied strain in the cycle is presented in Fig. 3. Each maximum applied strain corresponds to a unique crack density,  $\rho$ , value for each different material and lay-up. The procedure for its determination is described in Section 2. Alternatively, the measured stiffness reduction with strain and the theoretical model can be used to extract the corresponding crack density. Using these data and the data presented in Fig. 3, a diagram of the dissipated energy as a function of  $\rho$  for all experiments can be constructed.  $U_d$  versus transverse crack density is presented in Fig. 4.

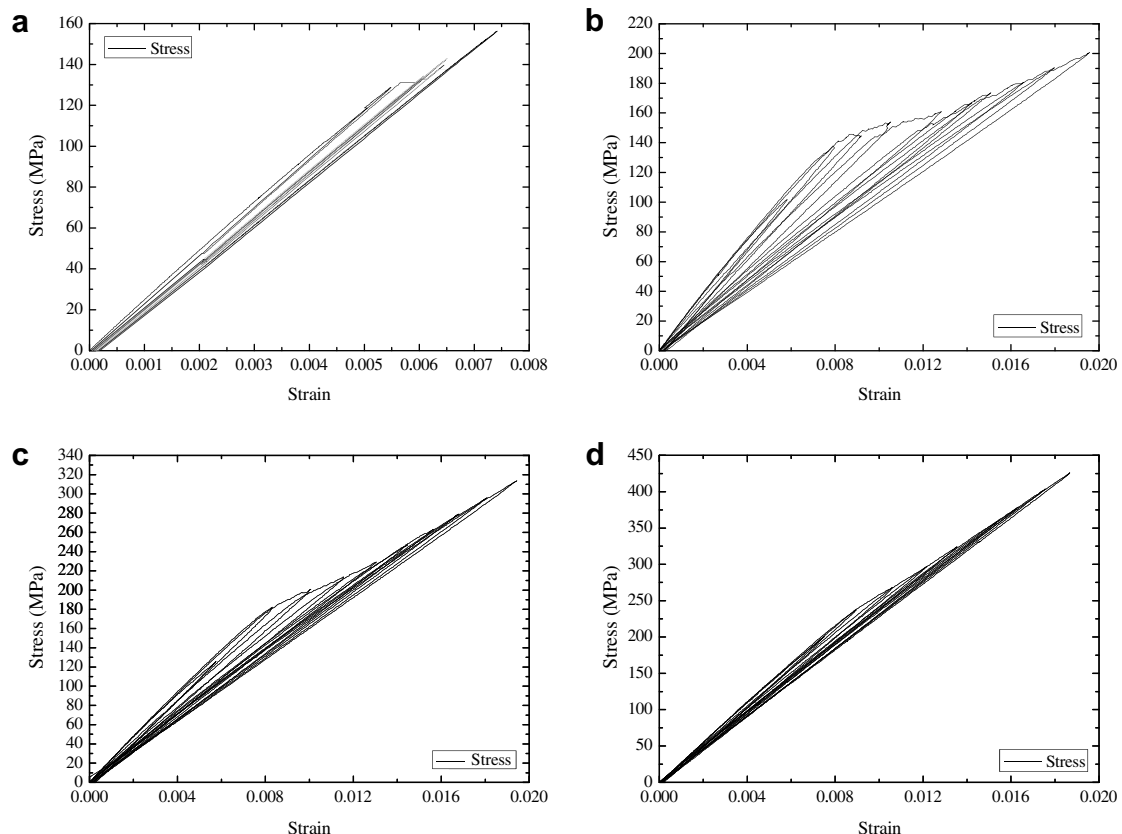


Fig. 2. Typical stress–strain curves for the two materials examined: (a) GF1, (b) GF2\_1-4, (c) GF2\_1-2 and (d) GF2\_2-2.



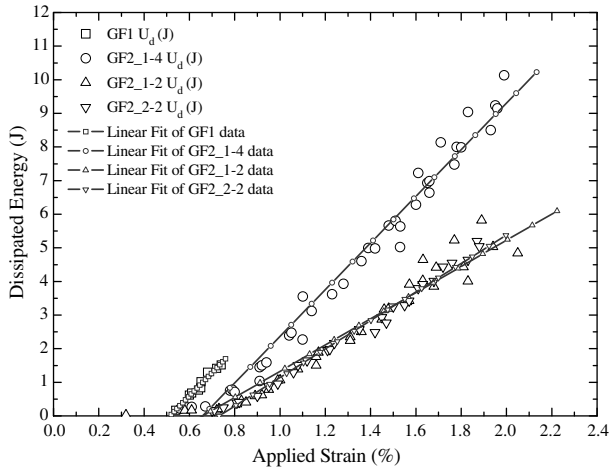


Fig. 3. Dissipated energy as a function of cycle maximum applied strain for all the materials tested.

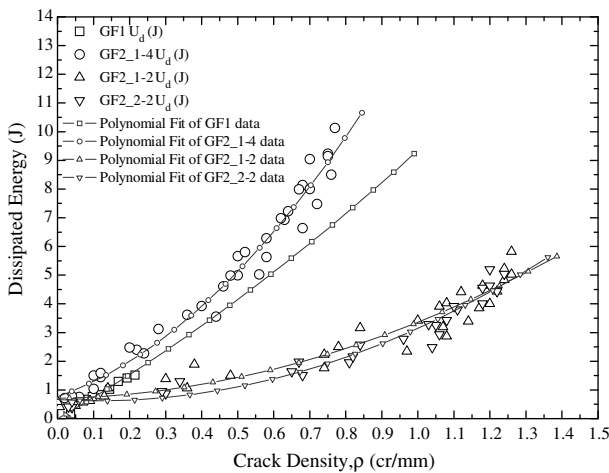


Fig. 4. The dissipated energy plotted against the modified crack density corresponding to each applied strain level for both materials systems.

Experimental  $G_c$  value is given by the total derivative of the dissipated energy,  $U_d$ , with respect to the total crack surface formed,  $A$

$$G_c = \frac{dU_d}{dA} \quad (16)$$

Polynomial fitting of the experimental data in Fig. 4 has been used in order to determine the  $G_c$  according to Eq. (16) for each different crack density value. The crack density,  $\rho$ , is related to  $A$  with expression (2), where  $N$  is the number of cracks formed that is related to  $\rho$  by (6). Using Eqs. (2), (6) and (16) the following expression, relating  $G_c$  with  $\rho$  through the actual 90°-layer volume,  $V_{90}$ , is constructed

$$G_c = \frac{1}{V_{90}} \frac{dU_d}{d\rho} \quad (17)$$

The critical strain energy release rate  $G_c$  as a function of  $\rho$  is presented in Fig. 5. Data presented in Fig. 5 possibly indicate that due to unstable growth more energy was re-

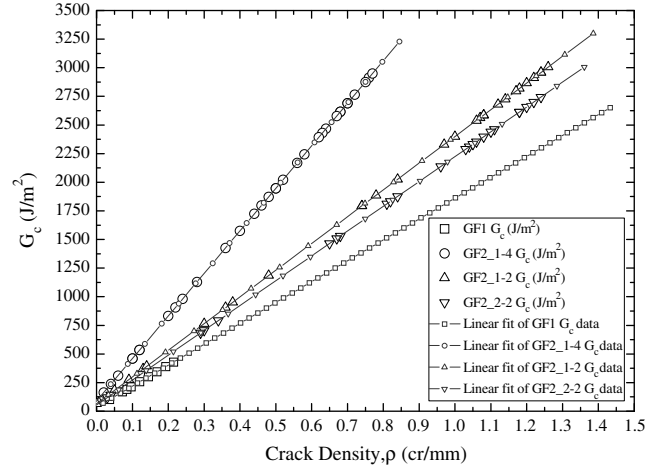


Fig. 5. Critical strain energy release rate as a function of the modified crack density.

leased than the actual required creating cracks in the GF2\_1-4 material. The difference becomes much smaller for the other two lay-ups with the same off-axis layer thickness. Inverting the previous strain-crack density procedure, i.e. going from cycle maximum applied strain to crack density, the relationship between  $G_c$  and the applied strain is extracted. The results are presented in Fig. 6. All the experimental data resulting from the three different GF2 laminates are plotted to show that the results could be considered laminate lay-up insensitive, while the dependence is different for GF1 and GF2 composites. In other words,  $G_c$  is a material characteristic and does not vary with ply thickness.

As an alternative approach we use the measured stiffness degradation with strain and Eq. (11) to calculate  $G_c$  corresponding to the given strain level (more exactly for cracks developing at this strain level). In derivation of (11) the results of previous works [7,26] on stiffness degradation

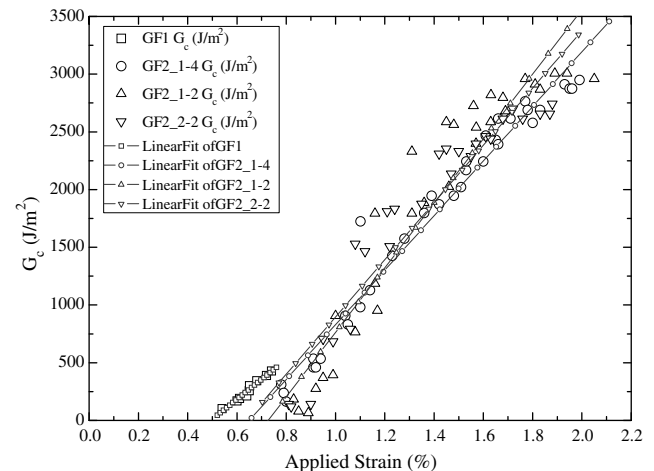


Fig. 6. Critical strain energy release rate as a function of applied strain. The data of the three different GF2 laminates are fitted by an average linear fitting curve.

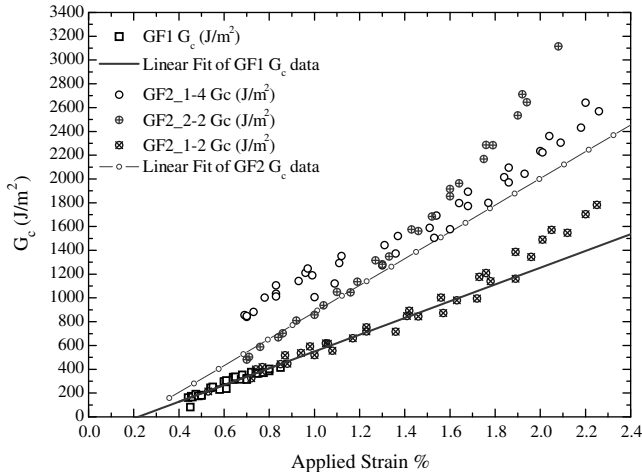


Fig. 7. Theoretical evaluation of the  $G_c$  as a function of maximum applied strain. GF2 data are considered as one data-set.

with increasing crack density have been used. The model proposed by Lundmark and Varna [26] has been proved to provide a very accurate description of the longitudinal Young's modulus relationship to the crack density. The  $G_c$  was calculated by Eq. (11) for every pair of points ( $\epsilon$ ,  $E_x$ ). The necessary pair of points can be easily found experimentally, from the corresponding stress–strain curves using the unloading curve as described. The results are presented in Fig. 7. An average linear fitting is used for all results from the three different GF2 laminates since  $G_c$  is considered as a fracture characteristic of a material not depending on geometrical characteristics. The rather linear behaviour of  $G_c$  with applied strain, which was observed in the dissipated energy calculations, see Fig. 6, is also presented here for the two different materials examined. The numerical values obtained using these two different techniques are rather close. Linear fit to these data was used as the first approximation in the following modelling. Certainly, more refined (bi-linear or S-shape) approximation would account for more details and would improve the predictions. However, the accuracy of the fitting has to be comparable with experimental differences between curves and the fact that  $G_c$  is considered as independent of the laminates lay-up.

$G_c$  for the GF2\_1-4 material calculated using the dissipated energy is used in order to develop an analytical method for simulation of the crack density corresponding to any applied strain level. Eq. (10) provides the requested relationship and, thus, it was used to derive theoretically the crack density as a function of the applied strain for all materials under consideration. The results are presented in Fig. 8 in comparison to experimentally derived crack density versus maximum applied strain data for both materials systems under investigation. Since new damage modes (blunted cracks, delta cracks, curved cracks, local delaminations, etc.) start to be dominant at strains higher than the so called “saturation state”, the described model for straight intralaminar cracks can not be used anymore. In

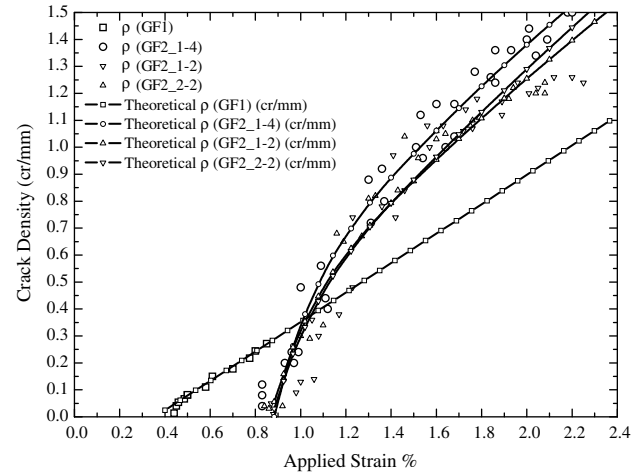


Fig. 8. Theoretical prediction of the crack density corresponding to applied strain level in comparison with experimentally derived data. The results are presented for both materials systems used.

order to extend the approach to this region these damage modes have to be classified, quantified and their effect on stiffness has to be modelled.

The experimental data, from the three different laminates manufactured using the GF2 material, are considered separately. The theoretical predictions appear to be in good agreement with the experimental data in the case of GF1 material. Considering the GF2 system three different predictions, with respect to the three different initial Young's moduli of the laminates are presented. The variation between the three different curves is not considerable, and all three are in agreement with the experimental data. Hence, in the crack density development the critical strain energy release rate can be treated as a material property to be calculated using macroscopically constructed stress–strain curves.

## 5. Conclusions

Critical strain energy release rate has been used as a means for the analytical prediction of the crack density arising in cross-ply composite laminates as a consequence of the external applied strain level. Two different GFRP material systems (GF1 and GF2) were used. GF2 system was used in three different stacking sequences with varying layer thickness ratio. The energy dissipated during all loading–unloading cycles was calculated using the recorded stress–strain curves. Together with experimental crack density evolution data for a reference laminate it was used in order to derive the  $G_c$  as a function of a crack density. This dependence represents the statistical nature of the composite fracture toughness,  $G_c$ , distribution (first cracks are in positions with lower fracture toughness). Using the reference lay-up crack density data the  $G_c$  was recalculated versus the corresponding tensile applied strain. A linear relationship between  $G_c$  and the maximum applied strain level was observed for both materials systems. This exper-

imental relationship was used for theoretical prediction of the crack density evolution with the applied strain in other laminates of the same material. An analytical model was used which requires only the material thermo-mechanical properties and the stiffness degradation law as a function of increasing crack density provided by any appropriate model. The theoretical calculations of the crack density as a function of the applied strain were compared to experimental data and a good agreement was found. It has been demonstrated that the energy dissipated during a loading–unloading cycle and the measured stiffness reduction can be used to determine  $G_c$  which can be treated as statistical material property and used in theoretical damage evolution models.

### Acknowledgements

Dr. S.L. Ogin and Mr. R.D. Whittingham of the University of Surrey are acknowledged for their contribution in the specimen manufacturing process as well as in the development of the whole project. Mr. E. Spārniņš and Dr. R. Joffe are acknowledged for conducting tensile experiments. D.T.G. Katerelos would like to acknowledge the Swedish Institute for granting a Guest post-doctoral scholarship during which this paper was developed.

### References

- [1] Talreja R. Damage characterization by internal variables. In: Pipes RB, Talreja R, editors. Composite materials series. Damage mechanics of composite materials, vol. 9. Amsterdam: Elsevier; 1994.
- [2] Varna J, Joffe R, Akshantala NV, Talreja R. Damage in composite laminates with off-axis plies. *Compos Sci Technol* 1999;59(14):2139–47.
- [3] Nairn J. Matrix microcracking in composites. In: Kelly A, Zweben C, Talreja R, Manson J-A, editors. Comprehensive composite materials. Polymer matrix composites, vol. 2. Amsterdam: Elsevier; 2000.
- [4] Berthelot J-M. Transverse cracking and delamination in cross-ply glass–fiber and carbon–fiber reinforced plastic laminates: static and fatigue loading. *Appl Mech Rev* 2003;56(1):111–47.
- [5] Kashtalyan M, Soutis C. Analysis of composite laminates with intra- and interlaminar damage. *Progr Aerosp Sci* 2005;41(2):152–73.
- [6] Katerelos DG, McCartney LN, Galiotis C. Local strain re-distribution and stiffness degradation in cross-ply polymer composites under tension. *Acta Mater* 2005;53(12):3335–43.
- [7] Katerelos DTG, Lundmark P, Varna J, Galiotis C. Analysis of matrix cracking in GFRP laminates using Raman spectroscopy. *Compos Sci Technol* 2006;67(9):1946–54.
- [8] Laws N, Dvorak GJ. Progressive transverse cracking in composite laminates. *J Compos Mater* 1988;22(10):900–16.
- [9] Lafarie-Frenot MC, Hénaff-Gardin C. Formation and growth of 90° ply fatigue cracks in carbon/epoxy laminates. *Compos Sci Technol* 1991;40(3):307–24.
- [10] Tong J, Guild FJ, Ogin SL, Smith PA. Off-axis fatigue crack growth and the associated energy release rate in composite laminates. *Appl Compos Mater* 1997;4(6):349–59.
- [11] Hénaff-Gardin C, Lafarie-Frenot MC. The use of a characteristic damage variable in the study of transverse cracking development under fatigue loading in cross-ply laminates. *Int J Fatigue* 2002;24(2–4):389–95.
- [12] Yokozeki T, Aoki T, Ishikawa T. Fatigue growth of matrix cracks in the transverse direction of CFRP laminates. *Compos Sci Technol* 2002;62(9):1223–9.
- [13] Li C, Ellyin F, Wharmby A. On matrix crack saturation in composite laminates. *Compos B Eng* 2003;34(5):473–80.
- [14] Caiazzo AA, Costanzo F. Modeling the constitutive behavior of layered composites with evolving cracks. *Int J Solids Struct* 2001;38(20):3469–85.
- [15] Rebière JL, Gamby D. Analytical and numerical analyses of transverse cracking in a cross-ply laminate – influence of the constraining effect. *Compos Struct* 1992;20(2):91–101.
- [16] Ogihara S, Takeda N, Kobayashi A. Experimental characterization of microscopic failure process under quasi static-tension in interleaved and toughness-improved CFRP cross-ply laminates. *Compos Sci Technol* 1997;57(3):267–75.
- [17] Anderssen R, Gradin PA, Gustafson CG. Prediction of the stiffness degradation in cross-ply laminates due to transverse matrix-cracking: an energy method approach. *Adv Compos Mater* 1998;7(4):325–46.
- [18] Ji FS, Dharani LR, Mall S. Analysis of transverse cracking in cross-ply composite laminates. *Adv Compos Mater* 1998;7(1):83–103.
- [19] Adolfsson E, Gudmundson P. Matrix crack initiation and progression in composite laminates subjected to bending and extension. *Int J Solids Struct* 1999;36(21):3131–69.
- [20] Ladevèze P, Lubineau G. On a damage Mesomodel for laminates: micro–meso relationships, possibilities and limits. *Compos Sci Technol* 2001;61(15):2149–58.
- [21] Yokozeki T, Aoki T, Ishikawa T. Consecutive matrix cracking in contiguous plies of composite laminates. *Int J Solids Struct* 2005;42(9–10):2785–802.
- [22] Smith PA, Ogin SL. On transverse matrix cracking in cross-ply laminates loaded in simple bending. *Compos A* 1999;30(8):1003–8.
- [23] Smith PA, Ogin SL. Characterization and modelling of matrix cracking in a (0/90)<sub>2s</sub> GFRP laminate loaded in flexure. *Proc Royal Soc Lond Ser A* 2000;456(2003):2755–70.
- [24] Crocker LE, Ogin SL, Smith PA, Hill PS. Intra-laminar fracture in angle-ply laminates. *Compos A* 1997;28(9–10):839–46.
- [25] Rubenis O, Spārniņš E, Andersons J, Joffe R. The effect of crack spacing distribution on stiffness reduction of cross-ply laminates. *Appl Compos Mater* 2007;14(1):59–66.
- [26] Lundmark P, Varna J. Constitutive relationships for laminates with ply cracks in in-plane loading. *Int J Damage Mech* 2005;14(3):235–59.
- [27] Wang ASD, Chou PC. A stochastic model for the growth of matrix cracks in composite materials. *J Compos Mater* 1984;18:239–54.